Journal of Molecular Biology
Volume 369, Issue 2, 1 June 2007, Pages 343-355
http://dx.doi.org/10.1016/j.jmb.2007.03.054

DNA Polymerase Switching on Homotrimeric PCNA at the Replication Fork of the Euryarchaea *Pyrococcus abyssi*

Christophe ROUILLON, Ghislaine HENNEKE, Didier FLAMENT, Joël QUERELLOU and Jean-Paul RAFFIN*

IFREMER, UMR 6197, Laboratoire de Microbiologie et Environnements Extrêmes, BP 70, F-29280 Plouzané, France.

* Corresponding author: Jean-Paul RAFFIN, Ifremer, EEP/LM2E, B.P. 70, 29280 Plouzané, France; Tel.: +33 2 98 22 45 39; Fax: +33 2 98 22 47 57;
E-mail: jpraffin@ifremer.fr

Abstract:

DNA replication in Archaea, as in other organisms, involves large protein complexes called replisomes. In the Euryarchaeota subdomain, only two putative replicases have been identified, and their roles in leading and lagging strand DNA synthesis are still poorly understood. In this study, we focused on the coupling of proliferating cell nuclear antigen (PCNA)-loading mechanisms with DNA polymerase function in the Euryarchaea *Pyrococcus abyssi*. PCNA spontaneously loaded onto primed DNA, and replication factor C dramatically increased this loading. Surprisingly, the family B DNA polymerase (Pol B) also increased PCNA loading, probably by stabilizing the clamp on primed DNA *via* an essential motif. In contrast, on an RNA-primed DNA template, the PCNA/Pol B complex was destabilized in the presence of dNTPs, allowing the family D DNA polymerase (Pol D) to perform RNA-primed DNA synthesis. Then, Pol D is displaced by Pol B to perform processive DNA synthesis, at least on the leading strand.

Keywords: Archaea; DNA replication; DNA polymerase switching; PCNA loading; RF-C

INTRODUCTION

DNA replication occurs by a functionally conserved mechanism in all organisms, including Bacteria, Eukarya, Archaea, and viruses,[1,2] and is tightly linked to the maintenance of genome stability.[3] DNA replication proceeds in three stages: initiation at the replication origins, DNA synthesis at the replication fork (elongation), and termination. Each of these processes involves different and successive stable or transient protein-protein and protein-DNA complexes; elongation depends on a large nucleoprotein assembly called the replisome.[4] DNA synthesis typically involves a protein triad composed of a clamp-loader, a sliding clamp, and a replicative DNA polymerase. In Eukarya and Bacteria, the clamp-loader catalyzes the assembly of the ring-shaped clamp around primer DNA in an ATP-dependent process; a replicative DNA polymerase is subsequently recruited and catalyzes highly processive DNA synthesis.[5,6] In Archaea, it has been reported that the clamp-loader does not require ATP hydrolysis to perform functional loading of the PCNA clamp.[7]

In *E. coli*, the chromosomal replicase is DNA polymerase III, and the three major functional units comprise ten different proteins.[8-10] The structures of the clamp (β)[11] and the clamp-loader (γ-complex)[12] are known. The replisome of the T4 bacteriophage, which involves a clamp (gp45), clamp-loader (gp44/gp62) and DNA polymerase (gp43), is also well characterized.[13-16]

A fascinating relationship was noted when the Eukarya and Archaea DNA replication proteins were compared. Complete sequencing of the archaeal genome[§], which is still an active field of study,[17] identified homologues of PCNA and RF-C, which are the eukaryal clamp and clamp-loader, respectively. Further, proteins involved in replication are functionally conserved throughout evolution, while sometimes showing little or no sequence similarity. Thus, DNA polymerase δ was shown to be stimulated by *Thermococcus fumicolans* PCNA,[18] the mammalian clamp-loader was able to interact with the *Pyrococcus furiosus* PCNA,[19] and

human PCNA could be loaded onto DNA by the *Pyrococcus abyssi* RF-C complex.[7] The archaeal DNA replication proteins are simpler than their eukaryal counterparts, i.e. there are fewer protein subunits involved. For example, the eukaryal RF-C complex has five different subunits,[20] the archaeal homologue has only two,[21-23] and the *Methanosarcina acetivorans* RF-C homologue is, uniquely, a three subunit clamp-loader.[24] In addition, the archaeal RF-C large subunit lacks a large part of the N-terminal sequence of the eukaryal homologue,[7] which should be taken into account when comparing the structures of the two clamp-loader complexes.[25-28]

Compared to their eukaryotic homologues, the archaeal replication factors display unique functional properties. Stimulation of archaeal DNA synthesis by PCNA on a circular DNA template was observed without the clamp-loader.[21,29,30] This was attributed to spontaneous loading that could be explained by weaker intermolecular interactions within PCNA monomers.[31] Moreover, the residues that maintain the toroidal structure of the archaeal PCNA were identified.[32] These results indirectly showed that the archaeal PCNA is able to load onto DNA in the absence of the clamp-loader.

When looking at the archaeal domain, it is clear that significant differences can be found within the main sub-domains, i.e. in the Euryarchaea and the Crenarchaea. Indeed, up to three PCNA homologues have been identified in Crenarchaea[30,33] that form a heterotrimer *in vivo*,[34] whereas only one homologue was found in Euryarchaea. In Archaea as well as in Eukarya and Bacteria, PCNA not only enhances the processivity of DNA replicases, but can also be conceptualized as a moving platform on which protein switches occur depending on the affinity of interacting factors, the structure of DNA, informational events, and cell cycle regulation.[35] Since PCNA is a trimer, it is possible that up to three protein factors could be bound at the same time. Alternatively, the factors may bind sequentially, depending on their functions during the cell cycle. In *E. coli*, protein–protein interaction studies demonstrated

that the DNA polymerase and clamp-loader actually bind to the same face of the clamp and, in fact, compete with one another.[36] It has been proposed that during Okazaki fragment maturation, proteins involved in this process compete for binding to the PCNA.[37,38] More recently, studies of the interplay between DNA replication and DNA repair suggest a modification of the composition and the processivity of the PCNA-protein complex, specifically the switching of the DNA polymerase involved in the process.[35,39-41] A DNA polymerase switch model was also described for the establishment of cohesion between sisters chromatids.[42]

Crenarchaea possess several (up to three) family B monomeric DNA polymerases [43,44] whereas Euryarchaea possesses one family B and one heterodimeric DNA polymerase belonging to family D that has only been found in this sub-domain.[45-48] We have previously shown that the two DNA polymerases from *P. abyssi*, *Pab*Pol B and *Pab*Pol D, were required for DNA replication and that only Pol D displayed RNA elongation and RNA strand-displacement activity in the presence of PCNA.[49] In the current study, we investigated PCNA-loading and recruitment of the two putative replicases. The subunit interactions within the complexes, coupled with functional studies, allows us to propose that DNA polymerase switching might occur on the loaded PCNA during euryarchaeal DNA replication.

RESULTS

*Pab*PCNA spontaneous loading on primed single-stranded DNA is enhanced at high temperature and reinforced by *Pab*RF-C and *Pab*Pol B.

Up to now, only indirect evidence suggested that archaeal PCNA could load spontaneously onto DNA. Therefore, we analyzed the loading of *Pab*PCNA onto different types of DNA substrate: short primed or non-primed 3'-5' biotinylated DNA template (ssDNA) or primed M13ssc. On the short synthetic substrate, loading was visualized in the absence of *Pab*RF-C (Figure 1(a)). Loading occurred on ssDNA (lanes 2-5) but was more efficient on primed DNA (lanes 6-9). Spontaneous loading of *Pab*PCNA onto primed ssDNA was increased at higher temperatures as demonstrated in Figure 1(b). Indeed, the loading efficiency at 37°C was only about 10% of that measured at 65°C. Moreover, including a non-biotinylated primed ssDNA as a competitor in the incubation dramatically reduced the loading efficiency: a six-fold reduction was observed at 65°C. This indicates that the *Pab*PCNA interaction with the DNA template is specific.

Spontaneous loading was also observed using the cross-linking method previously described for human PCNA[50] with a more physiological template, namely primed M13ssc DNA (Figure 2(a); see control, lane 2). *Pab*RF-C promoted the loading in the absence of ATP (Figure 2(a), lane 3), and either ATP or ATPγS increased the loading efficiency (Figure 2(a), lanes 4 and 5). However, semi-quantitative analysis clearly showed that ATP did not significantly stimulate the clamp-loading activity of *Pab*RF-C-promoted PCNA loading and that spontaneous loading was about 15% of the maximal loading efficiency in the presence of RF-C and ATPγS (Figure 2(c)).

To check the specificity of the loading, we next performed comparative studies with wild-type *Pab*PCNA and the triple mutant *Pab*PCNA(ded). This mutant could not trimerize (Figure 2(d)), and loading was defective in all conditions tested (Figure 2(a), lanes 6-9). This data was

supported by an experiment using fluorescently labeled molecules: DNA and *Pab*PCNA co-localize on the gel (Figure 2(b)). Indeed, when superposed, images acquired respectively at 488 and 532 nm showed co-localization of PCNA and DNA (yellow co-localization signal). In addition, these data confirmed the specific interaction observed between *Pab*RF-C and *Pab*PCNA loading onto DNA. We concluded that *Pab*PCNA was loaded as a homotrimer and that the technique used for measuring the loading was accurate.

When *Pab*Pol B was added to the loading reaction, spontaneous loading of *Pab*PCNA onto circular primed DNA was markedly increased (Figure 2(a), compare lanes 2 and 10, which show a 4-fold increase in loading). With *Pab*RF-C, some increase of loading was also observed, either in the presence (1.2-fold) or absence (2-fold) of ATP (Figure 2(a), compare lanes 3 and 11 and lanes 4 and 12), but not with ATPγS (Figure 2(a), compare lanes 5 and 13). In contrast, *Pab*Pol D did not enhance *Pab*PCNA loading (data not shown). Moreover, no signal was observed in the presence of *Pab*Pol B and *Pab*PCNA(ded), indicating that the DNA polymerase interacts only with the homotrimeric PCNA (data not shown).

Taken together, these data show that the trimeric form of *Pab*PCNA spontaneously loads onto DNA and that *Pab*RF-C, together with *Pab*Pol B, associates with the ring as a stable complex on primed DNA.

_Pab_PCNA/_Pab_Pol B are organized as a competent stable catalytic complex onto primed DNA, while the presence of an RNA primer is inhibitory.

Since *Pab*Pol B stimulated the binding and loading of *Pab*PCNA onto DNA, we added dNTPs into the loading reaction to determine whether a functional complex could form that was able to perform primer elongation. At first, when we used a higher resolution agarose gel, two loading populations were resolved (Figure 3(a)), and the addition of *Pab*Pol B increased the two loading forms on primed and non-primed M13ssc DNA (Figure 3(a), compare

respectively lanes 6 and 2 with lanes 10 and 11). However, while the signal was increased 9-fold on primed M13ssc (compare lanes 2 and 11), the increase was only 2-fold on non-primed DNA (compare lanes 6 and 10). When dNTPs were added to the incubation mixture, primer elongation was efficient. Primer elongation took place only with primed M13ssc DNA (Figure 3(a), compare lanes 12 and 13; Figure 3(b), lane 4), showing that a functional *Pab*PCNA/*Pab*Pol B complex formed only on the primed template. The primer elongation product was identified as the upper band, suggesting that the lower band was non-functional. Interestingly, in the presence of the *Pab*RF-C, only one broad, non-distinct band was visible (Figure 3(a), lanes 3-5 and 7-9).

Many DNA polymerases contain a conserved PCNA-binding motif (PIP-box) located at the C-terminus.[51] We deleted this motif in *Pab*Pol B and tested the ability of *Pab*Pol B(Δpip) to stimulate *Pab*PCNA loading. As shown in Figure 3(b), lanes 5 and 6, the *Pab*Pol B(Δpip) did not stimulate PCNA loading, and even suppressed spontaneous loading, probably by competing with PCNA on the primer-template junction.

*Pab*Pol B stimulated the loading of *Pab*PCNA onto RNA-primed DNA even more than onto the DNA-primed template: the signal increased 3-fold with the RNA primer (Figure 3(b), lanes 8 and 9) and only 1.5-fold with the DNA primer (Figure 3(b), lanes 2 and 3). Interestingly, addition of dNTPs abolished *Pab*Pol B-stimulated loading (Figure 3(b), lanes 9 and 10), and the observed signal was similar to that obtained with *Pab*PCNA alone (Figure 3(b), lane 8). This suggests that in the presence of an RNA-primed template, dNTPs destabilize the *Pab*Pol B/*Pab*PCNA complex.

_Pab_RF-C enhances DNA synthesis of short fragments by the _Pab_Pol B/PCNA complex but has no effect on the _Pab_Pol D/PCNA complex.

Thus far, we have shown that the *Pab*Pol B/*Pab*PCNA complex can be functionally loaded onto primed DNA without clamp-loading by *Pab*RF-C. To further investigate DNA synthesis in the presence of the two accessory proteins, we performed an *in vitro* DNA primer extension assay using *Pab*Pol B and *Pab*Pol D. First, we tested the ability of *Pab*PCNA to stimulate *Pab*Pol B DNA synthesis on primed M13ssc DNA. As shown in Figure 4(a), *Pab*PCNA clearly enhanced the extension activity of *Pab*Pol B in the absence of *Pab*RF-C. The phosphorylated *Pab*PCNA derivative was also active in promoting *Pab*Pol B DNA synthesis (Figure 4(a), lane 3), but the ph-*Pab*PCNA(ded) mutant was not active (Figure 4(a), lane 4). The *Pab*Pol B primer-extension assay was then performed in the presence of *Pab*RF-C (Figure 4b). Surprisingly, *Pab*RF-C favored the synthesis of short (< 2 kb) DNA fragments (Figure 4(b), lanes 2-3). The effect of *Pab*RF-C on releasing pausing sites in the 0.3-0.5 kb range and stimulating the accumulation of ~2 kb fragments was clearly visible when RF-C was added at different times during the incubation (Figure 4c). *Pab*PCNA also stimulated the primer-extension ability of *Pab*Pol D (Figure 4(b), lane 13). However, adding *Pab*RF-C to the reaction did not affect DNA synthesis by the *Pab*Pol D/*Pab*PCNA complex (Figure 4(b), lanes 14-16). Taken together, these data show that *Pab*RF-C affects the two *Pab* DNA polymerases differently, favoring DNA synthesis of short fragments by the Pol B/PCNA complex, while having no effect on the Pol D/PCNA complex.

We next performed a study of the interaction between *Pab*PCNA and *Pab*RF-C in order to determine the effect of ATP hydrolysis. The biotinylated primed 75-mer oligonucleotide was immobilized on streptavidin beads, and complexes with PCNA and RF-C were visualized by Western blot analysis with antibodies specific to *Pab*PCNA or to the *Pab*RF-C small subunit. On this short DNA substrate, PCNA loading was the same in the presence of *Pab*RF-C and either ATP or ATPγS (Figure 5(a), lanes 5-6). However, while *Pab*RF-C was part of the complex in the presence of ATPγS, the *Pab*RF-C signal was weaker in the presence of ATP

(Figure 5(b), compare lanes 5 and 6), showing that this factor was released upon completion of the loading process.

DNA polymerases compete for *Pab*PCNA independent of the presence of *Pab*RF-C.

Since *Pab*RF-C affected only the PCNA-stimulation and DNA synthesis of *Pab*Pol B, a competition between Pol B and the clamp-loader for interacting with the PCNA could occur. To investigate this hypothesis, we analyzed the interactions between the partners on a short primed 3'-5' biotinylated DNA template. The experiments were carried out with the same molar ratio for the different proteins, which were sequentially added to the reaction mixture. First, *Pab*PCNA, *Pab*RF-C, and the two *Pab* DNA polymerases interacted individually with the DNA template (Figure 6(a), lanes 5-8). In every case, the signal was higher than the background (Figure 6(b), compare lanes 5-8 to lanes 1-4). Second, *Pab*RF-C stimulated binding of *Pab*PCNA (Figure 6(a), compare lanes 5 and 9), resulting in about a 2-fold increase of the signal (Figure 6b). *Pab*Pol B, but not *Pab*Pol D, stimulated the binding of PCNA (Figure 6(a) and (b), lanes 5, 10, and 11) and *Pab*PCNA increased the binding of *Pab*Pol B (Figure 6(a) and (b), lanes 7 and 10) but not *Pab*Pol D (Figure 6(a) and (b), lanes 8 and 11). Third, *Pab*RF-C and *Pab*Pol B interacted together on the clamp (Figure 6(a), lane 13), showing that the inhibiting effect of *Pab*RF-C was not related to a PCNA-unloading mechanism. Surprisingly, in the presence of the DNA polymerase, the *Pab*RF-C was not released at the end of the loading process (Figure 6(a) and 6(b), lane 13), contrary to what was observed in the absence of *Pab*Pol B (Figure 5). In addition, RF-C was not released in the presence of the catalytic-competent complex Pol D/PCNA/DNA (Figure 6(a) and 6(b), lane 14). Interestingly, when mixing the two DNA polymerases together with PCNA and DNA, *Pab*Pol D could not form a stable catalytic complex with PCNA in the presence or the

absence of *Pab*RF-C (Figure 6(a) and 6(b), lanes 12 and 15), suggesting that the two *Pab* Pols compete for access to the PCNA platform.

DISCUSSION

The mechanism by which DNA polymerases achieve processivity is conserved among Prokarya, Eukarya, Archaea, and viruses. The DNA sliding clamp (the β subunit of DNA polymerase III holoenzyme in *E. coli*, gp45 in bacteriophage, and PCNA in Eukarya and Archaea) endows the replicative polymerase with high processivity. The clamp loader (the γ complex in *E. coli*, gp44/62 in T4 bacteriophage, and RF-C in Eukarya and Archaea) interacts with the clamp and uses ATP to drive clamp-loading onto primed DNA. The replicative DNA polymerases recruited for DNA synthesis are pol III in *E. coli*, pols δ and ε in Eukarya, at least one of three pols B in Crenarchaea, and pols B and D in Euryarchaea. When more than one replicative polymerase is present, questions about their involvement in leading or lagging strand synthesis have been raised.[52-55] For the Euryarchaea replication fork, the action of DNA polymerases has recently been investigated in *P. abyssi*.[49] Since only *Pab*Pol D, but not *Pab*Pol B, displayed PCNA-dependent RNA strand displacement in the conditions tested, it was assumed that both DNA polymerases were required for DNA replication in *P. abyssi*, with *Pab*Pol D involved at the lagging strand.

In this study, we investigated how the clamp-loading mechanism is coupled to DNA synthesis in the archaeon *P. abyssi*. We focused on mechanisms that could modulate the interaction of the two DNA polymerases, *Pab*Pol B and *Pab*Pol D, with the loaded *Pab*PCNA.

We first used cross-linking[50] and pull-down experiments to show that *Pab*PCNA spontaneously loaded onto synthetic short DNA templates as well as onto physiological DNA templates. Up to now, only indirect evidence had been obtained regarding the spontaneous loading of archaeal PCNA.[21] The loading was particularly efficient at high temperature (65°C) and with a primed template, which is in accordance with the physiological function of PCNA. By quantifying the amount of loaded PCNA, we found that about 15% loaded spontaneously compared to the amount loaded in the presence of *Pab*RF-C and ATPγS; the

clamp-loader was thus required for improving loading efficiency. As expected, no loading on any template was observed using mutant *Pab*PCNA defective in trimerization. This mutant PCNA was also unable to stimulate DNA synthesis by the DNA polymerases. Taken together, these data suggest that the RF-C is not required *in vivo* for loading of the archaeal PCNA. Interestingly, this implies that in Archaea, PCNA can be loaded onto circular DNA without energy (i.e. without ATP hydrolysis). Comparable results were obtained using primed M13 single-stranded DNA and the double biotinylated 75-mer, showing that spontaneous loading could not be attributed to the presence of linearized M13 DNA. In addition, the M13 circular DNA substrate was resistant to exonuclease VII digestion (results not shown). The self-loading of the archaeal PCNA could be due to the presence of additional ion pairs and fewer hydrogen bonds at the subunit interfaces.[31] In agreement with our data, it was previously shown that ATP hydrolysis by RF-C is not essential for either clamp loading onto DNA or the subsequent closing of the PCNA ring.[25] It has also been suggested that the RF-C open/PCNA open state could be transformed to the RF-C closed/PCNA closed state by the consumption of very little energy.[26] The existence of an equilibrium between open and closed PCNA could also explain the two bands we observe in the loading assay, with only one of them (the closed form) able to stimulate primer elongation (Figure 3). M13 DNA is highly structured,[56] and protein binding may influence its structure. This view is supported by the data in Figure 3, where very different migration properties are observed in the presence of RF-C.

Our second major observation was that the PCNA loading efficiency was boosted by *Pab*Pol B. In the loading assay with *Pab*Pol B, we observed a signal similar to that observed with the *Pab*RF-C complex, suggesting that once *Pab*Pol B interacts with PCNA, a very stable complex is formed on the DNA. This is similar to the situations previously described for the gp45 clamp with T4 DNA polymerase [57] and for the p125 subunit of DNA polymerase δ.[58] The clamp is thus stabilized on the DNA by the DNA polymerase.

The next question we addressed was what happens to the RF-C once the PCNA is loaded. We showed that in the presence of ATP, *Pab*RF-C is released from the complex with PCNA and DNA; however, in the presence of the DNA polymerase, RF-C remains in the complex. Our data raise an intriguing question about the synthesis of DNA fragments of reduced size by *Pab*Pol B and the *Pab*Pol B-PCNA complex with *Pab*RF-C. One hypothesis that can explain this phenomenon is non-specific DNA binding by the *Pab*RF-C complex. Indeed, it has been shown that human RF-C displays significant binding to DNA templates.[59-61] This strong and non-specific affinity is essentially due to the N-terminus of the p140 RF-C, which contains a DNA binding domain.[62,63] However, this N-terminal motif is lacking in the archaeal RF-C homologue.[7] The lack of strong non-specific DNA binding is reinforced by our results showing that *Pab*RF-C did not inhibit *Pab*Pol D DNA synthesis.

Previous studies have proposed that RF-C is interacting with PCNA when Pol δ binds to PCNA, suggesting that RF-C travels with Pol δ and PCNA.[64] Also in Archaea, the clamp-loader is presumed to be released from the loaded PCNA after ATP hydrolysis.[65] We show here that the picture could be different when DNA polymerases are present in the complex and that the RF-C could travel with the Pol and the PCNA during DNA synthesis. *Pab*Pols and *Pab*RF-C exhibit the consensus Pip motif (QVGLGAWLKF and QVTLFDFI, respectively) at the C-terminus, and *Pab*Pol B increased the loading of the PCNA via this motif. Therefore, more than one partner, but only one DNA polymerase, can bind to PCNA. At the C-terminus of all *Pyrococcus* RF-C large subunits, there is a 56 amino acid peptide sequence just in front of the PIP box that contains 49 charged amino acids (Lys, Glu, or Arg). This sequence might be poorly structured and could be a flexible connector between the PIP box and the main part of the *P. abyssi* large subunit. This cluster contains ten residues upstream of the PIP box that are important for stable binding to the PCNA [66]. Moreover, an interaction between the subunit DP1 of *Pho*Pol D and the large subunit of *Pho*RF-C has been

detected in *Pyrococcus horikoshii*.[67] Additional studies are required to elucidate the role of RF-C during archaeal DNA replication.

In the conditions tested, *Pab*Pol D is able to perform RNA primer extension and RNA strand displacement, whereas *Pab*Pol B is not.[49] This suggests that *Pab*Pol D could be required on both strands for elongation of the RNA primer and at the lagging stand to displace the downstream RNA primer. Here, we report a new DNA polymerase switching mechanism by which *Pab*Pol B displaces *Pab*Pol D from *Pab*PCNA on the DNA duplex. This switching could occur on both strands after RNA primer extension. On the other hand, *Pab*Pol B is unable to elongate a DNA primer if an RNA primer is located downstream up to 100 bases,[49] and we show here that the *Pab*Pol B/*Pab*PCNA complex was de-stabilized in the presence of an RNA primer and dNTPs. Considering that an archaeal Okazaki fragment length is up to 120 bases,[68] the RNA proximity would prevent the binding of *Pab*Pol B to *Pab*PCNA during RNA primer elongation by *Pab*Pol D, suggesting that the polymerase switching could occur during the late phases. It is possible that *Pab*Pol D could be required only for lagging strand synthesis, with polymerase switching at the leading strand leading to a very stable *Pab*Pol B/*Pab*PCNA complex via the *Pab*Pol B PIP box motif.

Acknowledgements

This work was supported by a grant from the European Union (Project # QLK3-CT-2002-02071 REPBIOTECH). The authors thank Audrey Le Goaziou for technical assistance.

MATERIALS AND METHODS

Chemicals and enzymes

We used the *P. abyssi* GE5 strain.[69] The genome of this organism was completely sequenced by Genoscope (Evry, France). *E. coli* DH5α and HMS174(DE3) cells were purchased from Clontech Laboratories (Basingtoke, UK) and Novagen (Madison, WI, USA), respectively. [γ-^{32}P]ATP (5000 Ci/mmol) was obtained from Amersham Biosciences (Saclay, France). Polyacrylamide gel electrophoresis (PAGE) reagents were obtained from BioRad (Ivry sur Seine, France). All other chemicals were molecular biology reagents from Sigma-Aldrich (St. Louis, MO, USA).

Nucleic acid substrates

Circular M13mp18 (M13ssc), either as single-stranded DNA or as primed single-stranded DNA, was obtained from Amersham Biosciences (Orsay, France). The primed substrate was obtained by annealing circular M13mp18 DNA to a DNA primer (5'-ATTCGTAATCATGGTCATAGCTGTTTCCTG-3') or to an RNA primer (5'-AUUCGUAAUCAUGGUCAUAGCUGUUUCCUG-3') at a 1:20 molar ratio, in 10 mM Tris-HCl pH 7.8, 125 mM NaCl and 2.5 mM $MgCl_2$, followed by heating at 90°C for 10 min and cooling to room temperature.

Recombinant proteins

The *P. abyssi* family B DNA polymerase (*Pab*Pol B) was the Isis™ DNA Polymerase commercialized by MP Biomedicals (Illkirch, France). *P. abyssi* family D DNA polymerase (*Pab*Pol D), *Pab*RF-C, and *Pab*PCNAwt were prepared as described earlier.[7,48] The mutant PCNA *Pab*PCNA(ded) was designed following results obtained with *Pyrococcus furiosus*.[32]

The amino acids E139, D143, and D147 were mutated to alanine by site-directed mutagenesis on the plasmid carrying the *Pab*PCNAwt gene[7] using the QuickChange™ Site-Directed Mutagenesis kit (Stratagene Europe, Amsterdam, The Netherlands). In order to obtain mutant PCNA derivatives carrying a phosphorylation site (ph-PCNA and ph-PCNA(ded)), a consensus amino acid sequence with a serine phosphorylable by HMK was introduced at the C-terminus of the protein.[50] HMS174(DE3) cells were transformed with the plasmids carrying the PCNA genes, and the proteins were expressed and purified as described previously.[7] Mutant *Pab*PCNA was constructed by mutating leucine 211 to a cysteine. A mutant version of *Pab*Pol B, with a deletion of the C-terminal PIP-box (Δpip) was obtained using the same mutagenesis protocol. The codon corresponding to lysine 759, just upstream of the PIP-box, was replaced by a stop codon. Recombinant proteins were expressed and purified as described previously.[48]

HPLC analysis

A Bio-Tek Kontron 520 chromatograph was used with a 535 detector operating at a wavelength of 280 nm. The flow cell was 8 µl and a loop injector was used to inject 20 µl. The column was a Superdex 200 PC (3.2 mm x 30 cm) with a mean particle size of 13 µm (Amersham Biosciences, Orsay, France). The buffer consisted of 50 mM Tris-HCl pH 7.5, 1 mM DTT, and 0.15 M NaCl, and the flow-rate was 40 µl/min. Thyroglobulin (669 kDa), ferritin (440 kDa), aldolase (158 kDa), ribonuclease A (137 kDa), bovine serum albumin (67 kDa), and ovalbumin (43 kDa) were used as molecular mass markers (Amersham Biosciences, Orsay, France).

Phosphorylation of ph-PCNA proteins

The ph-PCNA proteins were incubated for 20 min at 37°C in a 15 µl reaction containing 20 mM Tris-HCl pH 7.5, 1 mM DTT, 12 mM $MgCl_2$, 0.1 M NaCl, 12.5 nmole [γ-^{32}P] ATP, 1.15 µg of ph-PCNA or ph-PCNA(ded), and 2.25 Units of HMK (Sigma-Aldrich, St. Louis, MO, USA).

Fluorescent labeling of *Pab*PCNA(L211C)

*Pab*PCNA(L211C) reacted with TAMRA (Molecular Probes, OR, USA) in 20 mM Tris-HCl pH 7.0, 0.1 mM EDTA, in an oxygen-free environment according to the manufacturer's instructions. The reaction was allowed to proceed for 2 h and then 1 mM DTT was added. The labeled PCNA was purified sequentially on a 1 ml Resource Q column (Amersham Biosciences, Orsay, France) with stepwise elution with 1 M NaCl buffer, followed by desalting on a HiPrep 26/10 column (Amersham Biosciences, Orsay, France). An 80% yield of labeling was achieved.

Visualization of ph-PCNA/DNA complexes (cross-linking reaction)

The cross-linking reaction was carried out in 25 µl of loading buffer (20mM Hepes-NaOH pH 7.5, 2 mM DTT, 3 mM $MgCl_2$, 100 mM NaCl, 0.2 mg/ml BSA) containing 45 fmol of the nucleic acid substrate. Proteins were sequentially added as follows: 1.5 pmol of *Pab*RF-C, 1.6 pmol of *Pab*PCNA, and 0.1 pmol of *Pab*Pol B or 0.4 pmol of *Pab*Pol D. ATP or ATPγS were added at 1 mM final concentration and dNTPs at 0.4 mM. The reaction mixture was first incubated for 3 min at 65°C, then 2.5 µl of the cross-linking reagent glutaraldehyde at 1% (v/v) were added. The mixture was further incubated for 10 min at 65°C, and 5 µl of loading buffer (20 mM Tris-HCl pH 8, 1 mM EDTA, 50% glycerol and 0.07% bromophenol blue)

were added. The reaction mixture was then loaded onto a 0.8% agarose gel (TBE buffer containing 0.1% SDS) and electrophoresis was performed for 1-2 hours in the same buffer. The gel was then fixed with 10% trichloroacetic acid (10 min), rinsed two times in 10% acetic acid, 12% methanol (10 min), dried under a vacuum and finally revealed by autoradiography. Fluorescence imaging was made by using a *Pab*PCNA(L211C) labeled with tetramethylrhodamine and a M13ssc DNA primed with a 5'-fluorescein-labelled primer. Images were acquired on a Typhoon 9400 imager (Amersham Biosciences, Orsay, France).

Interactions studies using biotin-labeled DNA template coupled to streptavidin beads

A 48-mer oligonucleotide (5'-GAGTGCACGTTGACTACCCGTCTTGAGGCAGAGTCCG ACATCTAGCTC-3') was annealed to a 5'-
3' biotinylated 75-mer oligonucleotide (5'-biotGAGCTAGATGTCGGACTCTGCCTCAAGA CGGGTAGTCAACGTGCACTCGAGGTCATTTTTTTTTTTTTTTTTTTbiot-3') at equimolar ratio in a buffer containing 10 mM Tris-HCl pH 8.0, 1 mM EDTA, and 1 M NaCl. Next, 300 fmol of the biotinylated heteroduplex were incubated for 20 min with 20 µg of streptavidin beads. The beads were washed 3 times with in 10 mM Tris-HCl pH 8.0, 1 mM EDTA, 1 M NaCl. For one 25 µl reaction, 20 µg of beads loaded with the heteroduplex were resuspended in buffer (20 mM Hepes-NaOH pH 7.5, 2 mM DTT, 3 mM $MgCl_2$, 100 mM NaCl, and 0.2 mg/ml BSA). The reaction was then placed at 65°C, and pre-heated proteins were added to the mixture, with or without washing between additions. The amounts used were 0.24, 0.22, 0.29, and 0.22 pmol, respectively, of *Pab*RF-C, *Pab*PCNA, *Pab*Pol B, or *Pab*Pol D; ATP or ATPγS was added to a final concentration of 1 mM. The reaction was incubated for 3 min, and then the beads were washed three times with 1 ml of PBS, resuspended in loading buffer, and subjected to SDS-PAGE. After separation, proteins were transferred to nitrocellulose membranes. The blots were saturated with blocking buffer

containing 5% (w/v) skimmed milk in TBS-T (Tris-buffered saline: 10 mM Tris-HCl pH 7.5, 150 mM NaCl, 0.05% (v/v) Tween 20) for 30 min, then incubated for 2 h at room temperature with specific rabbit polyclonal antibodies directed against replication proteins (Eurogentec, Seraing, Belgium).

The membranes were washed three times with TBS-T, and then incubated for two hours with a 1:5,000 dilution of horseradish peroxidase-conjugated anti-rabbit antibody or 1:10,000 dilution of horseradish peroxidase-linked anti-mouse IgG in 2% (w/v) skimmed milk in TBS-T. The membranes were washed three times in TBS-T, and the secondary antibody was detected using enhanced chemiluminescence solution (SuperSignal® West Pico Chemiluminescence Substrate, Pierce, Rockford, IL, USA) according to the manufacturer's instructions.

Primer extension assays

The primer extension reactions (25 µl total volume) were incubated for 20 min at 65°C. Each reaction contained either 1.1 pmol of *Pab*Pol B in 50 mM Tris-HCl pH 8.0, 2 mM $MgCl_2$, 1 mM DTT, 10 mM KCl, 0.4 mg/ml BSA or else contained 2.3 pmol of *Pab*Pol D in 20 mM Bis-Tris pH 6.8, 10 mM $MgCl_2$, 1 mM DTT, 0.4 mg/ml BSA. Also included were 0.2 mM dNTPs, 3 µM of [α-^{32}P]dATP, 57 fmol of primed M13ssc DNA, 0.6 pmol of PCNA, 0.25 to 2.5 pmol of RF-C, and 0.5 mM of ATP or ATPγS. Loading buffer (3 µl containing 0.5 M NaOH, 10 mM EDTA, 25% Ficoll 400, and 0.25% bromophenol blue) was then added to the reaction mixture and products were resolved on 1.2% denaturing agarose gels at low temperature in a TAE 0.05x buffer containing 15 mM NaOH and 0.5mM EDTA. The gels were dried at room temperature and subjected to phosphorimaging analysis. A λ *Hind* III digest was labeled by incorporation of [α-^{32}P]dATP with Klenow fragments and used as molecular weight markers.

FIGURE LEGENDS

Figure 1: Loading of *Pab*PCNA onto a short DNA template. Pull-down experiments were performed as described in Materials and Methods with 300 fmol of the primed (sspDNA) or non-primed (ssDNA) 75-mer oligonucleotide immobilized on biotin beads. (a) Incubations were performed at 65°C for 3 min, in 25 µl of 20 mM Hepes-NaOH pH 7.5, 2 mM DTT, 3 mM $MgCl_2$, 100 mM NaCl, 0.2 mg/ml BSA, varying amounts of *Pab*PCNA, and 20 µg of beads carrying the heteroduplex. The products were analyzed on a 7.5% SDS-PAGE gel by Western blot with *Pab*PCNA antibodies. *Pab*PCNA was 0.06 (lanes 2 and 6), 0.6 (lanes 1, 3 and 7), 1.2 (lanes 4 and 8) or 2.4 (lanes 5 and 9) pmol. 'Input' is a positive control with 0.12 pmol of *Pab*PCNA. (b) Incubations were performed with 0.6 pmol of *Pab*PCNA and 3 fmol of competitor DNA (the primed non-biotinylated 75-mer). The incubation temperature is indicated at the top of the panel. Semi-quantitative densitometry analysis was performed on the gels. The highest band intensity for each experiment was considered to be the 100% value. These values are indicated underneath each panel. The molecular weight markers (M) were the ECL DualVue Western Blotting Markers from Amersham (Uppsala, Sweden).

Figure 2: Loading of *Pab*PCNA onto primed M13ssc DNA: effects of *Pab*RF-C and *Pab*Pol B. (a) The 25 µl reaction mixtures contained, in addition to buffer (see Materials and Methods), 45 fmol of primed M13ssc DNA (all reactions except lane 1); 1.8 pmol of [^{32}P]*Pab*PCNA (wild-type, wt, or mutant, ded); 1.2 pmol of *Pab*RF-C; 1 mM ATP or ATPγS; and 0.1 pmol of *Pab*Pol B as indicated for each lane. Reactions were incubated at 65°C for 3 min, and PCNA loading was measured by the cross-linking technique described in Materials and Methods. Lane 1 is a negative control lacking M13ssc DNA. (b) Co-localization of DNA and *Pab*PCNA on agarose gels. The reactions contained DNA (1) or DNA + PCNA (2). The excitation wavelength was 488 nm for fluorescein-labeled primed M13ssc DNA and 532 nm

for rhodamine-labeled *Pab*PCNA. On the right, the two images were superimposed, showing a yellow co-localization signal. The low intensity band for reaction 2 at 532 nm is due to some fluorescein signal at this wavelength (c) Semi-quantitative densitometry analysis of gels from six different experiments performed as described in Figure 2(a); the bands corresponding to conditions in lanes 2, 3, 4, and 5, respectively, in Figure 2(a), were quantified and the intensity of the ATPγS band (lane 5) was considered to be the 100% value. Error bars indicate the confidence level for the difference between the means ($\bar{X} \pm t_{\alpha/2} S_{\bar{X}}$), where α is the significance level used to compare the confidence level (0.05) and $t_{\alpha/2}$, the critical value from the t table with n-1 degrees of freedom.
(d) Superdex 200 PC chromatography of *Pab*PCNAwt and *Pab*PCNA(ded); conditions are described in Materials and Methods and the elution profiles correspond to the homotrimer *Pab*PCNAwt and the monomer *Pab*PCNA(ded), respectively

Figure 3: *Pab*Pol B-stimulated *Pab*PCNA loading: a functional complex forms on a primed DNA template. (a) The reaction mixtures are as described in Figure 2(a), including 1.8 pmol of [^{32}P]*Pab*PCNA in all reactions; either non-primed (M13ssc) or primed (pM13ssc) M13 single-stranded DNA; 1.2 pmol of *Pab*RF-C (lanes 3-5 and 7-9); 0.1 pmol of *Pab*Pol B (lanes 10-13), 1 mM ATP or ATPγS; and 0.4 mM dNTPs as indicated. PCNA loading was measured by cross-linking. (b) The reaction mixtures contained 45 fmol of DNA- or RNA-primed M13ssc DNA, as indicated at the bottom of the panel, and 1.8 pmol of [^{32}P]*Pab*PCNA. *Pab*RF-C was added with ATPγS and the quantities of *Pab*RF-C, *Pab*Pol B (or the PIP-box-deleted mutant *Pab*Pol B(Δpip)), dNTPs, and ATPγS are indicated in the legend to panel 3(a), above.

Figure 4: Primer elongation studies of *P. abyssi* DNA polymerases. The elongation reactions (see Materials and Methods) contained 1 pmol of *Pab*Pol B or 2.3 pmol of *Pab*Pol D, 56 fmol of primed M13ssc DNA, 2.4 pmol of *Pab*PCNA (wild-type, wt, or mutant, ded), 2 pmol of *Pab*RF-C, and 0.5 mM of ATP or ATPγS. Reactions were incubated at 65°C for 20 min, and products were resolved on 1.2% denaturing agarose gels and visualized by phosphoimaging analysis. Markers (M1 and M2) are *Hind* III digests of phage λ DNA labeled by incorporation of [^{32}P]dATP with the Klenow fragment. (a) Effect of wild-type and mutant *Pab*PCNA on *Pab*Pol B; 'ph-' indicates that the PCNA has a protein kinase consensus amino acid sequence at the C-terminus. (b) Effect of *Pab*RF-C and varying conditions on *Pab*Pol B (lanes 1-8) or *Pab*Pol D (lanes 9-16). (c) *Pab*RF-C was added at different times during the incubation, as indicated above the panel.

Figure 5: The stability of the *Pab*PCNA/*Pab*RF-C complex is modulated by ATP hydrolysis. Pull-down experiments were performed as described in Figure 1, and the products were analyzed by Western blot with antibodies to *Pab*PCNA (a) or to the small subunit of *Pab*RF-C (b). Lanes 1 and 2, controls with biotin immobilized on the beads; lanes 3-6, 300 fmol of primed 75-mer oligonucleotide were immobilized on 20 µg of streptavidin beads as described in Materials and Methods. Experiments were as follows. Lane 1, 2.4 pmol of *Pab*PCNA; lane 2, 2 pmol of *Pab*RF-C; lane 3, 2.4 pmol of *Pab*PCNA; lane 4, 2 pmol of *Pab*RF-C; lane 5, 2.4 pmol of *Pab*PCNA, 2 pmol of *Pab*RF-C, and 1 mM ATPγS; lane 6, 2.4 pmol of *Pab*PCNA, 2 pmol of *Pab*RF-C, and 1 mM ATP.

Figure 6: Physical interaction of *Pab*PCNA with DNA and proteins. Experiments were performed as described in Figure 1 with the biotinylated primed 75-mer oligonucleotide immobilized on streptavidin beads, except that 0.5 pmol of the indicated proteins were added.

When RF-C was present, 1 mM ATP was added. Products were analyzed by 7.5% SDS-PAGE. (a) Western blot using antibodies to *Pab*PCNA, the *Pab*RF-C small subunit, *Pab*Pol B, or the *Pab*Pol D small subunit, as indicated to the right of the panels. The positive control lane is labeled 'Input' with 0.01 pmol of *Pab*PCNA, 0.15 pmol of *Pab*RF-C, 0.06 pmol of *Pab*Pol B, or 0.04 pmol of *Pab*Pol D, respectively. (b) Semi-quantitative analysis of the data in Figure 6(a); for each gel, the highest band intensity was considered to be the 100% value.

REFERENCES

1. Forterre, P., Filée, J. & Myllykallio, H. (2004). Origin and evolution of DNA and DNA replication machineries. In *The Genetic Code and the Origin of Life* (de Pouplana, L. R., ed.), pp. 145-168. Kluwer Academic/Plenum Publishers, New York.
2. Kelman, Z. & O'Donnell, M. (1994). DNA replication: enzymology and mechanisms. *Curr. Opin. Genet. Develop.* **4**, 185-195.
3. Toueille, M. & Hübscher, U. (2004). Regulation of the DNA replication fork: a way to fight genomic instability. *Chromosoma* **113**, 113-125.
4. Kornberg, A. & Baker, T. A. (1992). Regulation of chromosomal replication and cell division. In *DNA replication* (Kornberg, A. & Baker, T. A., eds.), pp. 731-769. Freeman, New York.
5. Mossi, R. & Hübscher, U. (1998). Clamping down on clamps and clamp loaders - The eukaryotic replication factor C. *Eur. J. Biochem.* **254**, 209-216.
6. Bertram, J. G., Bloom, L. B., Hingorani, M. M., Beechem, J. M., O'Donnell, M. & Goodman, M. F. (2000). Molecular mechanism and energetics of clamp assembly in *Escherichia coli* - The role of ATP hydrolysis when γ complex loads β on DNA. *J. Biol. Chem.* **275**, 28413-28420.
7. Henneke, G., Gueguen, Y., Flament, D., Azam, P., Querellou, J., Dietrich, J., Hübscher, U. & Raffin, J. P. (2002). Replication Factor C from the hyperthermophilic archaeon *Pyrococcus abyssi* does not need ATP hydrolysis for clamp-loading and contains a functionally conserved RFC PCNA-binding domain. *J. Mol. Biol.* **323**, 795-810.
8. Johnson, A. & O'Donnell, M. (2005). Cellular DNA replicases: components and dynamics at the replication fork. *Annu. Rev. Biochem.* **74**, 283-315.

9. O'Donnell, M., Jeruzalmi, D. & Kuriyan, J. (2001). Clamp loader structure predicts the architecture of DNA polymerase III holoenzyme and RFC. *Curr. Biol.* **11**, R935-R946.

10. Onrust, R., Finkelstein, J., Naktinis, V., Turner, J., Fang, L. H. & Odonnell, M. (1995). Assembly of a chromosomal replication machine: Two DNA polymerases, a clamp loader, and sliding clamps in one holoenzyme particle .1. Organization of the clamps loader. *J. Biol. Chem.* **270**, 13348-13357.

11. Kong, X. P., Onrust, R., O'Donnell, M. & Kuriyan, J. (1992). Three-dimensional structure of the β subunit of E. coli DNA polymerase III holoenzyme: a sliding DNA clamp. *Cell* **69**, 425-437.

12. Jeruzalmi, D., O'Donnell, M. & Kuriyan, J. (2001). Crystal structure of the processivity clamp loader gamma (gamma) complex of E-coli DNA polymerase III. *Cell* **106**, 429-441.

13. Pietroni, P., Young, M. C., Latham, G. J. & Vonhippel, P. H. (1997). Structural analyses of gp45 sliding clamp interactions during assembly of the bacteriophage T4 DNA polymerase holoenzyme .I. Conformational changes within the gp44/62-gp45-ATP complex during clamp loading. *J. Biol. Chem.* **272**, 31666-31676.

14. Latham, G. J., Bacheller, D. J., Pietroni, P. & von Hippel, P. H. (1997). Structural Analyses of gp45 Sliding Clamp Interactions during Assembly of the Bacteriophage T4 DNA Polymerase Holoenzyme. II. The gp44/62 Clamp loader interacts with a single defined face of the sliding clamp ring. *J. Biol. Chem.* **272**, 31677-31684.

15. Latham, G. J., Bacheller, D. J., Pietroni, P. & Vonhippel, P. H. (1997). Structural analyses of gp45 sliding clamp interactions during assembly of the bacteriophage T4 DNA polymerase holoenzyme .III. The gp43 DNA polymerase binds to the same face of the sliding clamp as the clamp loader. *J. Biol. Chem.* **272**, 31685-31692.

16. Ishmael, F. T., Trakselis, M. A. & Benkovic, S. J. (2003). Protein-protein interactions in the bacteriophage T4 replisome - The leading strand holoenzyme is physically linked to the lagging strand holoenzyme and the primosome. *J. Biol. Chem.* **278**, 3145-3152.

17. Allers, T. & Mevarech, M. (2005). Archaeal genetics - The third way. *Nature Rev. Genet.* **6**, 58-73.

18. Henneke, G., Raffin, J. P., Ferrari, E., Jónsson, Z. O., Dietrich, J. & Hübscher, U. (2000). The PCNA from *Thermococcus fumicolans* functionally interacts with DNA polymerase delta. *Biochem. Biophys. Res. Commun.* **276**, 600-606.

19. Ishino, Y., Tsurimoto, T., Ishino, S. & Cann, I. K. (2001). Functional interactions of an archaeal sliding clamp with mammalian clamp loader and DNA polymerase δ. *Genes Cells* **6**, 699-706.

20. Yao, N. Y., Coyell, L., Zhang, D., Georgescu, R., Finkelstein, J., Coman, M. M., Hingorani, M. M. & O'Donnell, M. (2003). Replication Factor C clamp loader subunit arrangement within the circular pentamer and its attachment points to PCNA. *J. Biol. Chem.* **278**, 50744-50753.

21. Cann, I. K. O., Ishino, S., Hayashi, I., Komori, K., Toh, H., Morikawa, K. & Ishino, Y. (1999). Functional interactions of a homolog of proliferating cell nuclear antigen with DNA polymerases in Archaea. *J. Bacteriol.* **181**, 6591-6599.

22. Pisani, F. M., De Felice, M., Carpentieri, F. & Rossi, M. (2000). Biochemical characterization of a clamp-loader complex homologous to eukaryotic replication factor C from the hyperthermophilic archaeon *Sulfolobus solfataricus*. *J. Mol. Biol.* **301**, 61-73.

23. Seybert, A., Scott, D. J., Scaife, S., Singleton, M. R. & Wigley, D. B. (2002). Biochemical characterisation of the clamp/clamp loader proteins from the euryarchaeon *Archaeoglobus fulgidus*. *Nucl. Acids Res*. **30**, 4329-4338.

24. Chen, Y. H., Kocherginskaya, S. A., Lin, Y., Sriratana, B., Lagunas, A. M., Robbins, J. B., Mackie, R. I. & Cann, I. K. O. (2005). Biochemical and mutational analyses of a unique clamp loader complex in the archaeon *Methanosarcina acetivorans*. *J. Biol. Chem*. **280**, 41852-41863.

25. Miyata, T., Oyama, T., Mayanagi, K., Ishino, S., Ishino, Y. & Morikawa, K. (2004). The clamp-loading complex for processive DNA replication. *Nature Struct. Mol. Biol.* **11**, 632-636.

26. Miyata, T., Suzuki, H., Oyama, T., Mayanagi, K., Ishino, Y. & Morikawa, K. (2005). Open clamp structure in the clamp-loading complex visualized by electron microscopic image analysis. *Proc. Natl. Acad. Sci. USA* **102**, 13795-13800.

27. Lee, I., Lokanath, N. K., Min, K., Ha, S. C., Kim, D. Y. & Kim, K. K. (2002). Cloning, purification, crystallization and preliminary X-ray studies of RFC boxes II--VIII of replication factor C from *Methanococcus jannaschii*. *Acta Cryst. Ser. D* **58**, 519-521.

28. Bowman, G. D. (2004). Structural analysis of a eukaryotic sliding DNA clamp-clamp loader complex. *Nature* **429**, 724-730.

29. Kitabayashi, M., Nishiya, Y., Esaka, M., Itakura, M. & Imanaka, T. (2002). Gene cloning and polymerase chain reaction with proliferating cell nuclear antigen from Thermococcus kodakaraensis KOD1. *Biosci. Biotechnol. Biochem*. **66**, 2194-2200.

30. Daimon, K., Kawarabayasi, Y., Kikuchi, H., Sako, Y. & Ishino, Y. (2002). Three Proliferating Cell Nuclear Antigen-Like Proteins Found in the Hyperthermophilic

Archaeon *Aeropyrum pernix*: Interactions with the Two DNA Polymerases. *J. Bacteriol*. **184**, 687-694.

31. Matsumiya, S., Ishino, Y. & Morikawa, K. (2001). Crystal structure of an archaeal DNA sliding clamp: Proliferating Cell Nuclear Antigen from *Pyrococcus furiosus*. *Protein Sci.* **10**, 17-23.

32. Matsumiya, S., Ishino, S., Ishino, Y. & Morikawa, K. (2003). Intermolecular ion pairs maintain the toroidal structure of Pyrococcus furiosus PCNA. *Protein Sci.* **12**, 823-831.

33. De Felice, M., Sensen, C. W., Charlebois, R. L., Rossi, M. & Pisani, F. M. (1999). Two DNA polymerase sliding clamps from the thermophilic archaeon *Sulfolobus solfataricus*. *J. Mol. Biol*. **291**, 47-57.

34. Dionne, I., Nookala, R. K., Jackson, S. P., Doherty, A. J. & Bell, S. D. (2003). A heterotrimeric PCNA in the hyperthermophilic archaeon *Sulfolobus solfataricus*. *Mol. Cell* **11**, 275-282.

35. Maga, G. & Hübscher, U. (2003). Proliferating cell nuclear antigen (PCNA): a dancer with many partners. *J. Cell Sci.* **116**, 3051-3060.

36. Naktinis, V., Turner, J. & O'Donnell, M. (1996). A molecular switch in a replication machine defined by an internal competition for protein rings. *Cell* **84**, 137-145.

37. Lopez de Saro, F., Georgescu, R. E., Leu, F. & O'Donnell, M. (2004). Protein trafficking on sliding clamps. *Philos. Trans. R. Soc. Lond. Ser. B Biol. Sci.* **359**, 25-30.

38. Levin, D. S., Bai, W., Yao, N., Odonnell, M. & Tomkinson, A. E. (1997). An interaction between DNA ligase I and proliferating cell nuclear antigen: Implications for Okazaki fragment synthesis and joining. *Proc. Natl. Acad. Sci. USA* **94**, 12863-12868.

39. Plosky, B. S. & Woodgate, R. (2004). Switching from high-fidelity replicases to low-fidelity lesion-bypass polymerases. *Curr. Opin. Genet. Develop.* **14**, 113-119.

40. Friedberg, E. C., Lehmann, A. R. & Fuchs, R. P. P. (2005). Trading Places: How Do DNA Polymerases Switch during Translesion DNA Synthesis? *Mol. Cell* 18, 499-505.

41. Lehmann, A. R. (2006). Translesion synthesis in mammalian cells. *Exp. Cell Res.* **312**, 2673-2676.

42. Carson, D. R. & Christman, M. F. (2001). Evidence that replication fork components catalyze establishment of cohesion between sister chromatids. *Proc. Natl. Acad. Sci. USA* **98**, 8270-8275.

43. Cann, I. K. O., Ishino, S., Nomura, N., Sako, Y. & Ishino, Y. (1999). Two family B DNA polymerases from *Aeropyrum pernix*, an aerobic hyperthermophilic crenarchaeote. *J. Bacteriol.* **181**, 5984-5992.

44. Iwai, T., Kurosawa, N., Itoh, Y. H., Kimura, N. & Horiuchi, T. (2000). Sequence analysis of three family B DNA polymerases from the thermoacidophilic crenarchaeon *Sulfurisphaera ohwakuensis*. *DNA Res.* **7**, 243-251.

45. Cann, I. K. O., Komori, K., Toh, H., Kanai, S. & Ishino, Y. (1998). A heterodimeric DNA polymerase: Evidence that members of Euryarchaeota possess a distinct DNA polymerase. *Proc. Natl. Acad. Sci. USA* **95**, 14250-14255.

46. Ishino, Y. & Cann, I. K. O. (1998). The euryarchaeotes, a subdomain of Archaea, survive on a single DNA polymerase: Fact or farce? *Genes Genet. Syst.* **73**, 323-336.

47. Shen, Y., Musti, K., Hiramoto, M., Kikuchi, H., Kawarabayashi, Y. & Matsui, I. (2001). Invariant Asp1122 and Asp1124 are essential residues for polymerization catalysis of family D DNA polymerase from *Pyrococcus horikoshii*. *J. Biol. Chem.* **276**, 27376-27383.

48. Gueguen, Y., Rolland, J. L., Lecompte, O., Azam, P., Le Romancer, G., Flament, D., Raffin, J. P. & Dietrich, J. (2001). Characterization of two DNA polymerases from the hyperthermophilic euryarchaeon *Pyrococcus abyssi*. *Eur. J. Biochem.* **268**, 5961-5969.

49. Henneke, G., Flament, D., Hübscher, U., Querellou, J. & Raffin, J. P. (2005). The Hyperthermophilic Euryarchaeota *Pyrococcus abyssi* Likely Requires the Two DNA Polymerases D and B for DNA Replication. *J. Mol. Biol.* **350**, 53-64.

50. Podust, L. M., Podust, V. N., Sogo, J. M. & Hübscher, U. (1995). Mammalian DNA polymerase auxiliary proteins: Analysis of replication factor C-catalyzed proliferating cell nuclear antigen loading onto circular double-stranded DNA. *Mol. Cell Biol.* **15**, 3072-3081.

51. Warbrick, E. (1998). PCNA binding through a conserved motif. *Bioessays* **20**, 195-199.

52. Waga, S. & Stillman, B. (1998). The DNA replication fork in eukaryotic cells. *Annu. Rev. Biochem.* **67**, 721-751.

53. Hübscher, U., Maga, G. & Spadari, S. (2002). Eukaryotic DNA polymerases. *Annu. Rev. Biochem.* **71**, 133-163.

54. Shcherbakova, P. V., Bebenek, K. & Kunkel, T. A. (2003). Functions of eukaryotic DNA polymerases. *Sci. Aging Knowl. Environ.* **2003**, RE3.

55. Fukui, T., Yamauchi, K., Muroya, T., Akiyama, M., Maki, H., Sugino, A. & Waga, S. (2004). Distinct roles of DNA polymerases δ and ε at the replication fork in *Xenopus* egg extracts. *Genes Cells* **9**, 179-191.

56. Reckman, B., Grosse, F., Urbanke, C., Frank, R., Blöcker, H. & Krauss, G. (1985). Analysis of secondary structures in M13mp18(+) single-stranded DNA by the pausing of DNA polymerase α. *Eur. J. Biochem.* **152**, 633-643.

57. Yao, N., Turner, J., Kelman, Z., Stuckenberg, P. T., Dean, F. B., Shechter, D., Pan, Z. Q., Hurwitz, J. & O'Donnell, M. (1996). Clamp-loading, unloading and intrinsic stability of the PCNA, beta and gp45 sliding clamps of human, *E. coli* and T4 replicases. *Genes Cells* **1**, 101-113.

58. Zhang, P., Mo, J. Y., Perez, A., Leon, A., Liu, L., Mazloum, N., Xu, H. & Lee, M. (1999). Direct interaction of proliferating cell nuclear antigen with the p125 catalytic subunit of mammalian DNA polymerase δ. *J. Biol. Chem.* **274**, 26647-26653.

59. Lee, S. & Hurwitz, J. (1990). Mechanism of Elongation of Primed DNA by DNA Polymerase δ, Proliferating Cell Nuclear Antigen, and Activator 1. *Proc. Natl. Acad. Sci. USA* **87**, 5672-5676.

60. Tsurimoto, T. & Stillman, B. (1991). Replication factors required for SV40 DNA replication *in vitro*. I. DNA structure-specific recognition of a primer-template junction by eukaryotic DNA polymerases and their accessory proteins. *J. Biol. Chem.* **266**, 1950-1960.

61. Keller, R. C., Mossi, R., Maga, G., Wellinger, R. E., Hübscher, U. & Sogo, J. M. (1999). Electron microscopic analysis reveals that replication factor C is sequestered by single-stranded DNA. *Nucl. Acids Res.* **27**, 3433-3437.

62. Burbelo, P. D., Utani, A., Pan, Z. Q. & Yamada, Y. (1993). Cloning of the large subunit of activator 1 (replication factor C) reveals homology with bacterial DNA ligases. *Proc. Natl. Acad. Sci. USA* **90**, 11543-11547.

63. Fotedar, R., Mossi, R., Fitzgerald, P., Rousselle, T., Maga, G., Brickner, H., Messier, H., Khastilba, S. & Hübscher, U. (1996). A conserved domain of the large subunit of replication factor C binds PCNA and acts like a dominant negative inhibitor of DNA replication in mammalian cells. *EMBO J.* **15**, 4423-4433.

64. Yuzhakov, A., Kelman, Z., Hurwitz, J. & O'Donnell, M. (1999). Multiple competition reactions for RPA order the assembly of the DNA polymerase δ holoenzyme. *EMBO J.* **18**, 6189-6199.

65. Barry, E. R. & Bell, S. D. (2006). DNA Replication in the Archaea. *Microbiol. Mol. Biol. Rev.* **70**, 876-887.

66. Nishida, H., Ishino, S., Miyata, T., Morikawa, K. & Ishino, Y. (2005). Identification of the critical region in replication factor C from Pyrococcus furiosus for the stable complex formation with proliferating cell nuclear antigen and DNA. *Genes Genet. Syst.* **80**, 83-93.

67. Tang, X. F., Shen, Y., Matsui, E. & Matsui, I. (2004). Domain Topology of the DNA Polymerase D Complex from a Hyperthermophilic Archaeon *Pyrococcus horikoshii*. *Biochemistry USA* **43**, 11818-11827.

68. Matsunaga, F., Norais, C., Forterre, P. & Myllykallio, H. (2003). Identification of short 'eukaryotic' Okazaki fragments synthesized from a prokaryotic replication origin. *EMBO Rep.* **4**, 1-5.

69. Erauso, G., Reysenbach, A. L., Godfroy, A., Meunier, J. R., Crump, B., Partensky, F., Baross, J. A., Marteinsson, V., Barbier, G., Pace, N. R. & Prieur, D. (1993). *Pyrococcus abyssi* sp. nov., a new hyperthermophilic archaeon isolated from a deep-sea hydrothermal vent. *Arch. Microbiol.* **160**, 338-349.

Figure

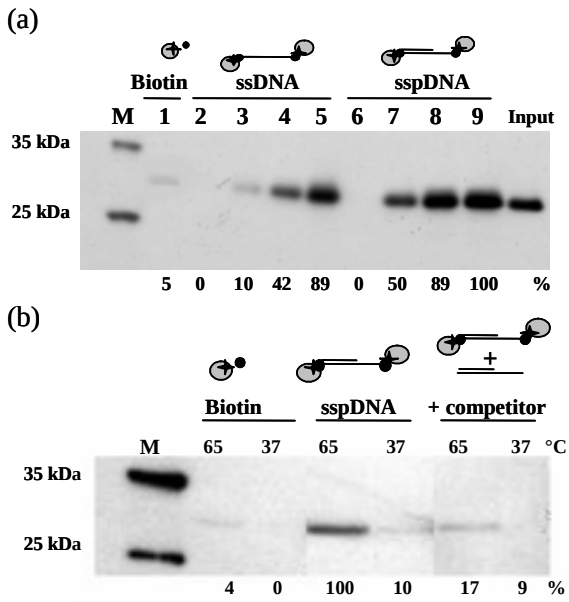
(a)
Biotin
ssDNA
sspDNA
M 1 2 3 4 5 6 7 8 9 Input
35 kDa
25 kDa
5 0 10 42 89 0 50 89 100 %
(b)
+
Biotin
sspDNA
+ competitor
M 65 37 65 37 65 37 °C
35 kDa
25 kDa
4 0 100 10 17 9 %

Figure

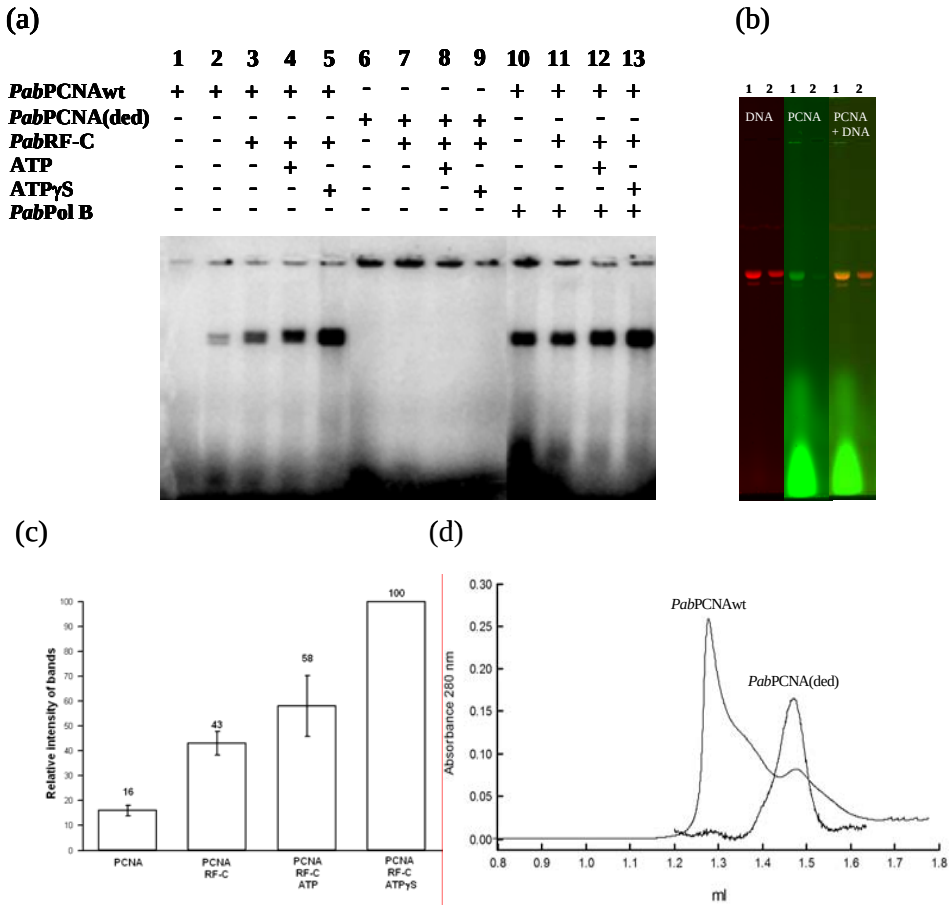
(a)
1 2 3 4 5 6 7 8 9 10 11 12 13
PabPCNAwt + + + + + - - - - + + + +
PabPCNA(ded) - - - - - + + + + - - - -
PabRF-C - - + + + - + + + - + + +
ATP - - - + - - - + - - - + -
ATPγS - - - - + - - - + - - - +
PabPol B - - - - - - - - - + + + +
(b)
1 2 1 2 1 2
DNA
PCNA
PCNA + DNA
(c)
Relative intensity of bands
16
43
58
100
PCNA
PCNA RF-C
PCNA RF-C ATP
PCNA RF-C ATPγS
(d)
Absorbance 280 nm
PabPCNAwt
PabPCNA(ded)
ml

Figure

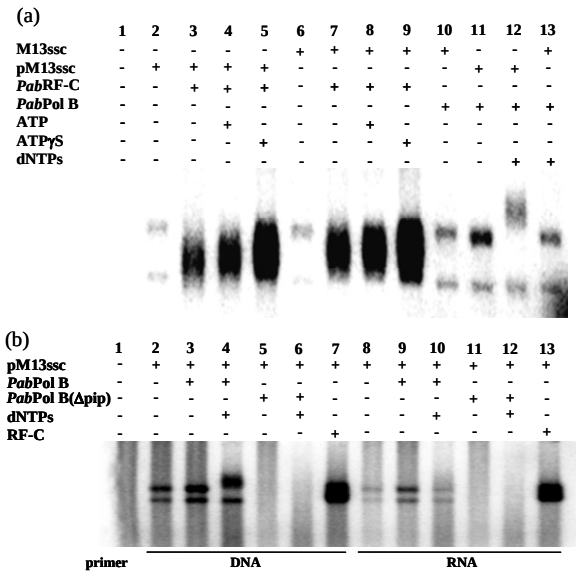
(a)
1 2 3 4 5 6 7 8 9 10 11 12 13
M13ssc - - - - - + + + + + - - +
pM13ssc - + + + + - - - - - + + -
PabRF-C - - + + + - + + + - - - -
PabPol B - - - - - - - - - + + + +
ATP - - - + - - - + - - - - -
ATPγS - - - - + - - - + - - - -
dNTPs - - - - - - - - - - - + +
(b)
1 2 3 4 5 6 7 8 9 10 11 12 13
pM13ssc - + + + + + + + + + + + +
PabPol B - - + + - - - - + + - - -
PabPol B(Δpip) - - - - + + - - - - + + -
dNTPs - - - + - + - - - + - + -
RF-C - - - - - - + - - - - - +
primer
DNA
RNA

Figure

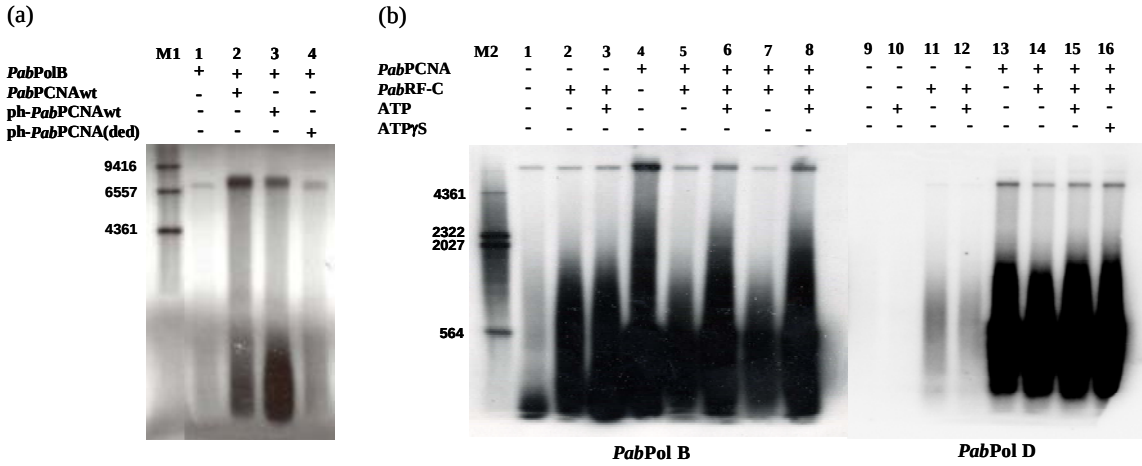
(a)
M1 1 2 3 4
PabPolB + + + +
PabPCNAwt - + - -
ph-PabPCNAwt - - + -
ph-PabPCNA(ded) - - - +
9416
6557
4361
(b)
M2 1 2 3 4 5 6 7 8 9 10 11 12 13 14 15 16
PabPCNA - - - + + + + + - - - - + + + +
PabRF-C - + + - + + + + - - + + - + + +
ATP - - + - - + - + - + - + - - + -
ATPγS - - - - - - - - - - - - - - - +
4361
2322
2027
564
PabPol B
PabPol D

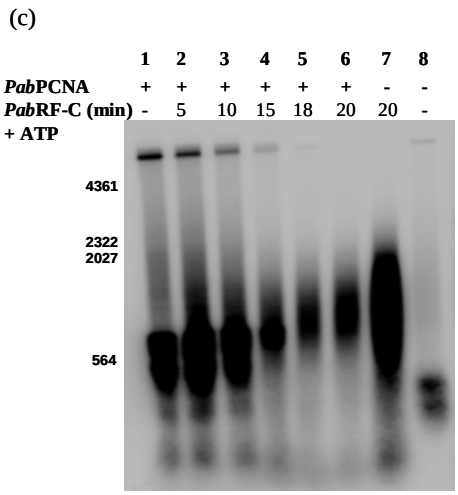
(c)
1 2 3 4 5 6 7 8
PabPCNA + + + + + + - -
PabRF-C (min) - 5 10 15 18 20 20 -
+ ATP
4361
2322
2027
564

Figure

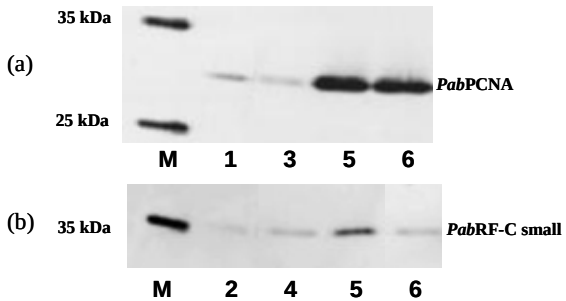

Figure

(a)

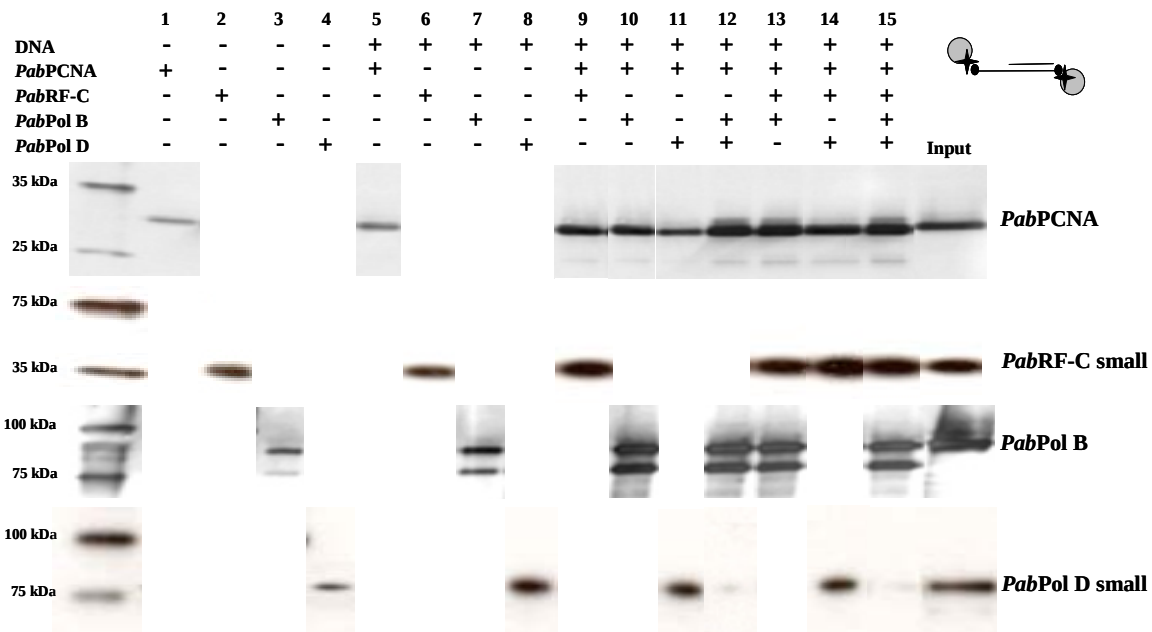
1 2 3 4 5 6 7 8 9 10 11 12 13 14 15
DNA - - - - + + + + + + + + + + +
PabPCNA + - - - + - - - + + + + + + +
PabRF-C - + - - - + - - + - - - + + +
PabPol B - - + - - - + - - + - + + - +
PabPol D - - - + - - - + - - + + - + +
Input
35 kDa
25 kDa
PabPCNA
75 kDa
35 kDa
PabRF-C small
100 kDa
75 kDa
PabPol B
100 kDa
75 kDa
PabPol D small

Figure

(b)

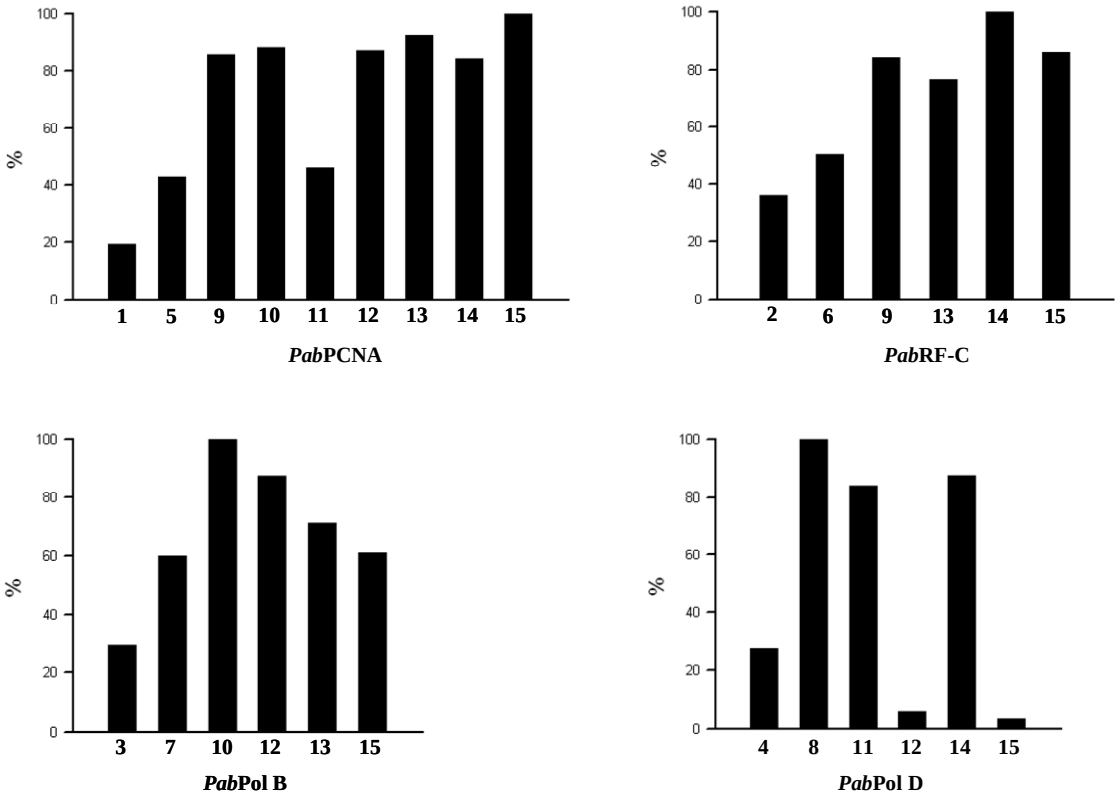
100
80
60
40
20
0
%
1 5 9 10 11 12 13 14 15
*Pab*PCNA
2 6 9 13 14 15
*Pab*RF-C
3 7 10 12 13 15
*Pab*Pol B
4 8 11 12 14 15
*Pab*Pol D